Case Studies in Concept Exploration and Selection with s-Pareto Frontiers

C.A. Mattson*
Department of Mechanical Engineering,
Brigham Young University, Provo UT, USA
E-mail: mattson@byu.edu
*Corresponding author

A.A. Mullur
Upstream Research Company,
ExxonMobil, Houston TX, USA
E-mail: anoop.a.mullur@exxonmobile.com

A. Messac
Department of Mechanical and Aerospace Engineering,
Rensselaer Polytechnic Institute,
Troy NY, USA
E-mail: messac@rpi.edu

Abstract: This paper investigates three disparate design cases where the newly developed *s-Pareto frontier based concept selection paradigm* is used to compare competing design concepts under a multiobjective optimization framework. The new paradigm, which was recently introduced by the authors, is based on the principle of Pareto optimality – a principle that defines an important class of optimal solutions to multiobjective optimization problems. These solutions, termed Pareto solutions, are optimal in the sense that improvement in one objective can only occur with the worsening of at least one other. The set of Pareto solutions comprises the Pareto frontier – a frontier that is particularly useful in engineering design because it characterizes the tradeoffs between the design objectives. Under the newly developed paradigm, a so-called *s-Pareto frontier* is used to characterize the tradeoffs between conflicting design objectives *and* the tradeoffs between competing design concepts. As such, the s-Pareto frontier holds significant potential for the important activity of concept selection. In this paper, the usefulness of the s-Pareto frontier for concept evaluation and selection is explored through examining three real-world case studies. As such, the present paper takes a needed and notable step beyond the simple two and three bar truss examples provided by the authors in previous archival publications on the s-Pareto topic. The first case study considers the design of a battery contact for a mobile phone; the second case involves the design of a compliant bicycle derailleur; the third involves the design of a rigidified inflatable structure. Each case provides a unique perspective on the s-Pareto frontier based concept selection paradigm.

Keywords: multiobjective optimization; s-Pareto frontier; pareto frontier; tradeoff analysis; compliant mechanism; rigidified inflatable structures.

Reference to this paper should be made as follows: Mattson, C.A., Mullur, A.A., (200X) 'Case Studies in Concept Exploration and Selection with s-Paerto Frontiers', Int. J. of Product Development, Vol. X, Nos. XX, pp.XX–XX.

Biographical notes: Christopher A. Mattson is Assistant Professor of Mechanical Engineering at Brigham Young University (PhD 2003, Rensselaer Polytechnic Institute). Anoop A. Mullur is Senior Research Engineer at ExxonMobil (PhD 2005, Rensselaer Polytechnic Institute). Achille Messac is Professor of Mechanical and Aerospace Engineering at Rensselaer Polytechnic Institute (PhD 1986 Massachusetts Institute of Technology).

1 Nomenclature

Γ_i	The goodness of the i-th design concept
g	Vector of inequality constraints
h	Vector of equality constraints
μ	Vector of design objectives (or design metrics)
μ^{*k}	Optimum design objective value for concept k
n	Number of design objectives
n_c	Number of design concepts
n_s	Number of s-Pareto solutions
n_{si}	Number of s-Pareto solutions originating from the i-th concept
n_x	Number of design variables
RI_i	The i-th Region of Interest
x	Vector of design variables

Subscripts and Superscripts

$*$	Indicates "optimal"
k	Indicates "the k-th concept"
l	Lower bound
u	Upper bound
s	Indicates "the set of concepts"

2 Introduction

The process of designing a product or system generally requires the designer to make tradeoffs between conflicting design objectives. Identifying the best balance between these objectives is one of the designer's most challenging and important tasks. We note that this task bears an additional layer of complexity in the early phases of design – when various distinct design concepts are still under evaluation. Identifying the tradeoffs for a set of disparate design concepts, in addition to considering the conflicting nature of the design objectives, is the substance of this added complexity. Notwithstanding, the success and competitiveness of the final design is critically dependent on the designer's ability to characterize these design tradeoffs and navigate through the design options.

One particular design tool that has proven effective in managing the tradeoffs between competing design objectives is Multiobjective Optimization (MO)(1; 2; 3). Though typically used during the latter phases of design (after a basic design concept has been chosen), MO has allowed designers to rapidly and effectively identify final optimal designs. As a result, MO has become widely used and highly valued in engineering design.

An important class of solutions to the MO problem is said to belong to the Pareto frontier. Each solution comprising the Pareto frontier is optimal in the sense that improving the performance of one design objective results in the worsening of at least one other objective (1). A two-dimensional Pareto frontier, for a minimization problem, is shown in Fig. 1(a). The design objectives are labeled μ_1 and μ_2, and are represented along each axis of the plot.

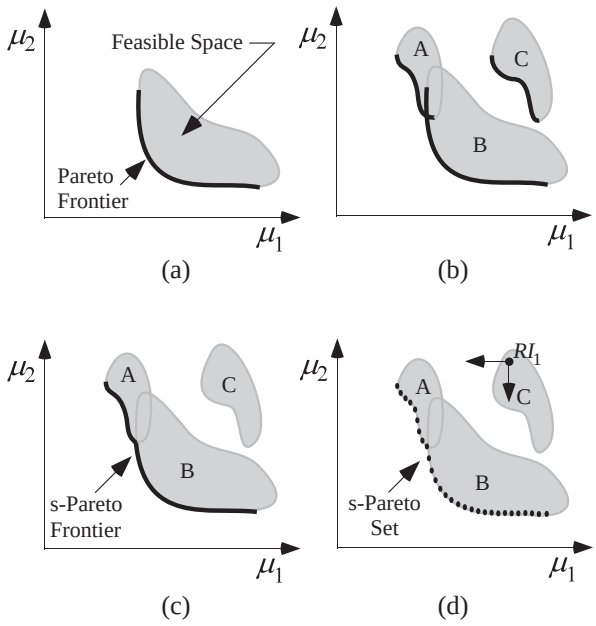

Figure 1: (a) The feasible space (shaded) and Pareto frontier (bold curve) for a generic design concept. (b) The Pareto frontiers for three disparate concepts. (c) The s-Pareto frontier, or Pareto frontier for the set of three concepts. (d) A set of s-Pareto solutions.

The shaded region represents the feasible design space for a generic design concept, and the heavy curve represents that concept's Pareto frontier.

The Pareto frontier plays a significant role in engineering design because it characterizes the tradeoffs between the design objectives. Whether the designer chooses a strategy that results in a single optimal solution, or one that results in a set of optimal solutions from which to subjectively choose a final design, the obtained solutions desirably belong to the Pareto frontier (4; 5; 6).

Because the MO process is not typically invoked until detailed design – after a basic design concept has already been chosen – the overall success of the MO process depends on the effectiveness of the approach used to select the basic concept that will be optimized. Therefore, we note that the process of evaluating disparate design concepts, and selecting the one that merits refinement, is a key step in the design process. When compared to the rigorous nature of MO, common approaches for concept evaluation/selection (such as voting (7), feasibility judgement (8), Quality Function Deployment (9), and the Pugh concept selection method (10; 7)) can be viewed as inadequately suited to sufficiently explore the tradeoffs for a set of design concepts (11).

In an effort to improve the effectiveness of conceptual design activities, there has been an increased thrust to develop concept selection approaches that capitalize on the benefits of multiobjective optimization. Ramaswamy et al. use MO in conceptual design to identify promising combinations of subsystems in multi-system design (12). Crossley et al. use a genetic algorithm and combinatorial

optimization to select basic aircraft concepts in conceptual design (13). Perez et al. take a similar approach to aircraft conceptual design, using adaptive genetic algorithms (14). Simpson uses MO approaches for feature selection in product family design (15). The work is extended by Pedersen (16) and later in Messac et al. (17; 18) by using the Physical Programming optimization approach. Topology optimization has also been used during conceptual design to determine the design layout, structurally (19).

In a recent publication (20), we presented a new Pareto frontier-based approach to concept selection in conceptual engineering design. Under the new framework, disparate design concepts are evaluated using a so-called *s-Pareto frontier*; this frontier originates from the Pareto frontiers of various disparate concepts, and *is* the Pareto frontier for the *set* of concepts.

Consider the three generic design concepts shown in Fig. 1(b) as shaded regions; the concepts are labeled A, B, and C. Each of these concepts has a Pareto frontier, which is shown as a bold curve. When comparing these concepts, it can be seen that Concept A is superior in minimizing objective μ_1, Concept B is superior in minimizing μ_2, and that Concept C is inferior to both Concepts A and B. The s-Pareto frontier, shown as a bold curve shown in Fig. 1(c), characterizes the tradeoffs between these concepts. The s-Pareto frontier also characterizes the tradeoffs between the design objectives. These properties of the s-Pareto frontier make it extremely useful for decision-making in conceptual design – where decisions have a significant impact on the design success (21; 20; 22; 23; 24).

Important additional developments to the s-Pareto frontier-based concept selection framework include the consideration of uncertainty, the quantification of concept goodness, and methods for visualizing n-dimensional s-Pareto frontiers (11; 25; 26).

In this paper, three real-world case studies are used to examine the applicability of the s-Pareto frontier based concept selection framework. As such, the present paper takes a needed and notable step beyond the simple two and three bar truss examples provided by the authors in previous archival publications on the s-Pareto topic (11; 25). Each case study illustrates a different aspect of the newly developed framework. The first case study is the design of a battery contact for a mobile phone. The purpose of this study is to illustrate the basic s-Pareto frontier based concept selection framework and show how it fits into a typical conceptual design process. The second case study is the conceptual design of a compliant bicycle derailleur. The purpose of this study is to illustrate how the s-Pareto frontier can be used to characterize tradeoffs in objectives and concepts, when the objective space is more than two dimensions and therefore not easily visualized. The third, and final, case study considers the design of a complex system – a rigidified inflatable structure. This case study shows that the new framework can be used to evaluate complex systems, and that (depending on the nature of the design problem) a minimal number of s-Pareto solutions can be obtained and used to approximate the s-Pareto frontier. In each case studies, the s-Pareto frontier proves useful in characterizing design tradeoffs and navigating through the design options.

The remainder of the paper is divided into five major parts; Sections 3–7. In Sec. 3, a brief overview of the s-Pareto frontier based concept selection framework is provided. In Sec. 4, 5, and 6, the case studies are presented; design of a battery contact, design of a compliant bicycle derailleur, and the design of a rigidified inflatable structure, respectively. Concluding remarks are provided in Sec. 7.

3 The s-Pareto concept selection framework

In this section, we present a brief overview of the s-Pareto frontier based concept selection framework, hereafter referred to as the *s-Pareto framework*. This section is divided into two major parts. In the first, we consider the generic multiobjective optimization (MO) problem (Problem 1) and the associated Pareto frontier. In the second part, we consider the MO problem statement when various disparate design concepts are involved (Problem 2). Under the latter, the resulting s-Pareto frontier plays an important role in evaluating the disparate concepts.

3.1 Generic Multiobjective Optimization

The generic multiobjective optimization problem is stated below in Problem 1.

Problem 1: Generic Multiobjective Optimization

$$\min_x [\ \mu_1(x)\ \ \mu_2(x)\ \cdots\ \mu_n(x)\ ]^T \tag{1}$$

subject to

$$g(x) \leq 0 \tag{2}$$

$$h(x) = 0 \tag{3}$$

$$x_{il} \leq x_i \leq x_{iu} \qquad (i = 1, 2, ..., n_x) \tag{4}$$

where μ_i is the i-th design metric, g and h are vectors of inequality and equality constraints, respectively, and x is a vector of design variables, bound by the lower and upper limits, which are denoted as x_l and x_u, respectively. The number of design objectives and design variables are respectively denoted as n and n_x.

As formulated, Problem 1 yields a set of solutions that belong to the Pareto frontier of a generic design concept, such as that shown in Fig. 1(a). Typically, the final design alternative is chosen from a set of generated points on the Pareto frontier.

3.2 Optimization-based Concept Selection

We now consider the generic MO problem statement when various disparate design concepts are involved. For clarity, we carefully describe our use of the terms *design alternative* and *design concept*. A design *concept* is a basic idea

that has evolved to the point where there is a parametric model that represents a family of specific design *alternatives* that belong to that concept's definition. Figure 1 is again used to provide a graphical perspective. Fig. 1(b) shows three basic design concepts, labeled A, B, and C. The feasible region (shaded) of each concept is defined by that concept's parametric model, however rudimentary it may be. Each specific design within each concept is termed a design alternative. For example, any point on the Pareto frontier of Concepts A, B, or C is a Pareto optimal design alternative (for that concept). The culminating event of conceptual design is the selection of one or more basic concepts that merit further development in the detailed design stage. Whereas, the culminating event of detailed design is the identification of a final design alternative that will typically go into production.

The s-Pareto frontier for the set of concepts shown in Fig. 1(b) is illustrated by the heavy curve in Fig. 1(c). Each solution comprising the s-Pareto frontier is said to be *s-Pareto optimal*, which means there are no other designs – from the same or any other concept – for which all objectives are better. Formally, we define s-Pareto optimality as follows.

s-Pareto Optimality: A design objective vector μ^{s*} is s-Pareto optimal if there does not exist another design objective vector μ^k in the feasible design space of concept k such that $\mu_i^k \leq \mu_i^{s*}$ for all $i \in \{1, 2, ..., n\}$ and all concepts k, where $k \in \{1, 2, ..., n_c\}$; and $\mu_j^k < \mu_j^{s*}$ for at least one j, $j \in \{1, 2, ..., n\}$ for any concept k, $k \in \{1, 2, ..., n_c\}$. The number of design concepts is denoted by n_c, and the number of design objectives is denoted as n.

The "s" in *s-Pareto frontier* indicates that the Pareto frontier is for the *set* of concepts. Similar to other Pareto frontiers, the s-Pareto frontier can be used to determine the tradeoffs between design objectives. *However, unlike other Pareto frontiers, the s-Pareto frontier can be used to characterize the tradeoffs between design concepts.* We make the important observation that unlike decision matrix based methods where concept selection is based on a single performance value for the objectives, the s-Pareto framework accounts for the objectives behaviors over ranges.

The multiobjective optimization problem statement that yields the s-Pareto frontier is stated below in Problem 2.

Problem 2: Obtaining the s-Pareto frontier

$$\min_k \left\{ \min_{x^k} \left[\mu_1^k(x^k) \;\; \mu_2^k(x^k) \;\; \cdots \;\; \mu_n^k(x^k) \right]^T \right\} \tag{5}$$

subject to

$$g^k(x^k) \leq 0 \tag{6}$$

$$h^k(x^k) = 0 \tag{7}$$

$$x_{il}^k \leq x_i^k \leq x_{iu}^k \qquad i = 1, ..., n_x \tag{8}$$

where

$$x^k = \left[x_1^k \;\; ... \;\; x_{n_x^k}^k \right]^T \tag{9}$$

and k, $k \in \{1, 2, ..., n_c\}$, denotes the k-th concept, μ^k is a vector containing design metrics for concept k, and x^k denotes the design variable vector for concept k.

Various approaches may be used to obtain a set of points that discretely represents the s-Pareto frontier. This set, referred to as the s-Pareto set, is illustrated in Fig. 1(d). Approaches for obtaining the s-Pareto set include the following: (i) Obtaining Pareto sets for each concept (using any Pareto set generator), and filtering out any solution that does not satisfy the definition of s-Pareto optimality. (ii) Directly obtaining the s-Pareto set using a single optimization problem statement. The latter is discussed in detail in Mattson and Messac (20). The method presented in Mattson and Messac (20) yields a set of evenly distributed points along the s-Pareto frontier, not unlike the distribution of points illustrated in Fig. 1(d). We note that by even distribution, we mean that no one part of the Pareto frontier is over or under represented in the Pareto set.

Once the s-Pareto frontier has been obtained, the process of using it to identify the dominance disposition of the candidate concepts can begin. A useful approach for doing this is to (i) define a *region of interest*, and (ii) quantify the goodness of each concept within that region. This approach is described in detail in Mattson and Messac (11). A terse description of the basic approach is given here.

The designer evaluates the goodness of the concepts within a particular region of the design space that is of interest to him or her. We call this a *Region of Interest*. The region southwest of the point RI_1 in Fig. 1(d) is an example of a region of interest. By exploring various regions of interest, the designer can start to collect information about the design space (i.e., which concepts occupy which parts of the design space); this information is then used to identify the concept or concepts that merit further development.

In evaluating concept goodness, we examine Pareto frontier surface areas and assume that concepts whose Pareto frontiers have larger surface areas potentially offer more design *flexibility* than those with smaller Pareto surface areas. More flexible concepts are assumed to be preferred because they provide more design freedom for detailed design.

As described in Mattson and Messac (11), the goodness of each concept is quantified by determining the intersection of a concept's Pareto frontier with the s-Pareto frontier. Mathematically, the goodness of the i-th concept is expressed as

$$\Gamma_i = \frac{\int_{S_p \cap S_{pi}} dS_p}{\int_{S_p} dS_p} \tag{10}$$

where S_p is the s-Pareto frontier, and S_{pi} is the Pareto frontier for the i-th concept. The numerator and denominator in Eq. 10 are n dimensional integrals. Equation 10

denotes the fraction of the s-Pareto frontier that originates from the i-th concept. An approximation of this goodness measure is now provided for the discrete domain. Given a set of evenly distributed points along the s-Pareto frontier, this measure of goodness is conveniently expressed as

$$\Gamma_i \approx \frac{n_{si}}{n_s} \tag{11}$$

where n_s is the total number of s-Pareto solutions and n_{si} be the number of s-Pareto solutions originating from the i-th concept. An interactive design space exploration tool, introduced in Mattson and Messac, allows the designer to intuitively change the region of interest; with each change made to the region of interest, the measure of concept goodness is automatically updated (11). This interactive approach has been particularly helpful in exploring s-Pareto frontiers of three or more dimensions. For a comprehensive description of the s-Pareto frontier-based concept selection framework see Mattson and Messac (20; 11), and Mattson (26).

In the following sections, we examine the usefulness of the s-Pareto frontier for concept selection. Specifically, we examine three unique design cases – each illustrating a different and important aspect of the s-Pareto framework. In Sec. 4, the s-Pareto frontier is used to evaluate and select a promising concept for a mobile phone battery contact. This example illustrates the framework in a two objective context. In Sec. 5, the design of a compliant bicycle derailleur is presented. The purpose of this study is to examine the s-Pareto framework in a three objective context. Finally, in Sec. 6, the s-Pareto frontier is used in the conceptual design of a rigidified inflatable structure. For the latter, it is specifically used to evaluate and select candidate materials for the inflatable structure.

4 Case Study 1: Battery Contact for Phone

In this section, we consider the design of a small component for a mobile phone – a battery contact. The purpose of this case study is to illustrate the basic elements of the s-Pareto framework, and how it fits into the conceptual design process. We begin this section with the basic contact design problem, followed by a description of the candidate contact concepts. We then provide the multiobjective optimization problem statement, the results thereof, and a brief discussion.

Battery contacts are continually adapting to meet the market's demand for smaller mobile electronic devices such as mobile phones. To maintain a reliable electrical connection in these smaller devices, sufficient contact deflection and contact normal force must now be achieved in smaller connector packages. This poses a notable challenge to the miniaturization of these devices. Multiple-bend contacts, such as those shown in Fig. 2, can be a good approach for achieving acceptable normal forces and deflections in small packages. This case study focuses on the design of this type of contact.

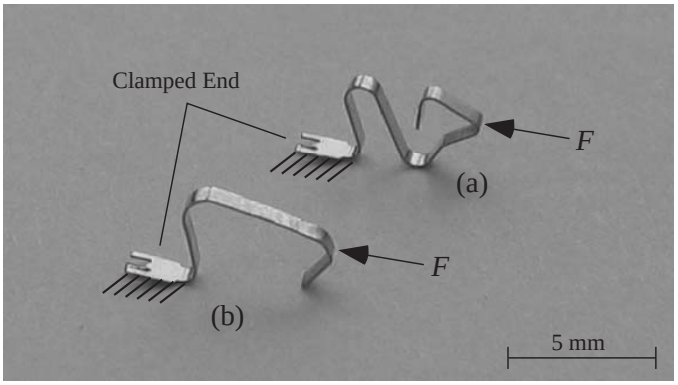

Figure 2: (a,b) Multiple-bend battery contacts for mobile devices.

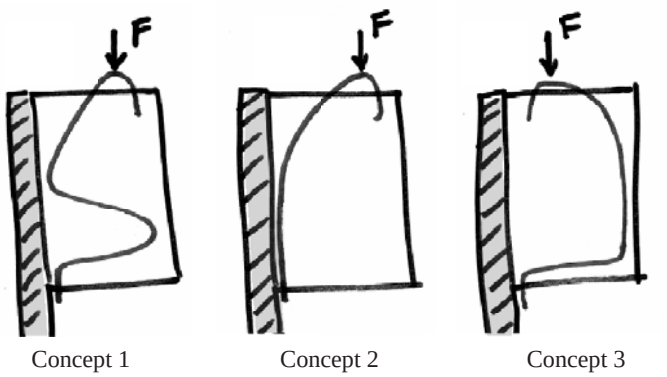

Figure 3: Conceptual sketches of three battery contact concepts considered in case-study.

Battery Contact Design Problem: Design a progressive-die-formed battery contact that experiences maximum deflections and minimal bending stresses for a prescribed contact normal force (F). Additionally, the profile (side-view) of the contact must fit in a 5 mm by 10 mm window.

4.1 Candidate Battery Contact Concepts:

Three designer-generated concepts for the battery contact are expressed conceptually in Fig 3. As shown in the figure, the curved line represents the profile of the contact; the hatched region represents a cross-section of a circuit board to which the contact is fixed; and the box enclosing the contact represents a plastic connector housing. We note that it is for simplicity of presentation that we consider a small number of concepts in this case study. Under the s-Pareto framework, any number of concepts could be considered.

After having generated these contact concepts, the designer must now evaluate and select the most promising design based on the objectives of minimizing bending stress and maximizing deflection in the direction of the prescribed load F. While many designers are capable of intuitively predicting the behavior of these concepts, it is generally not possible to do so over the full range of behaviors that can be obtained by perturbing the geometry

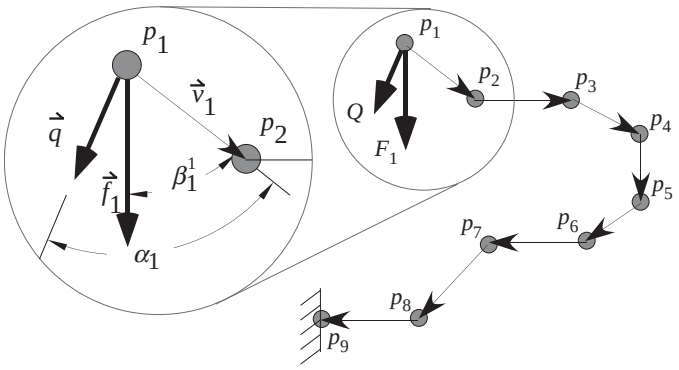

Figure 4: Simplified geometric vector model of a generic contact concept

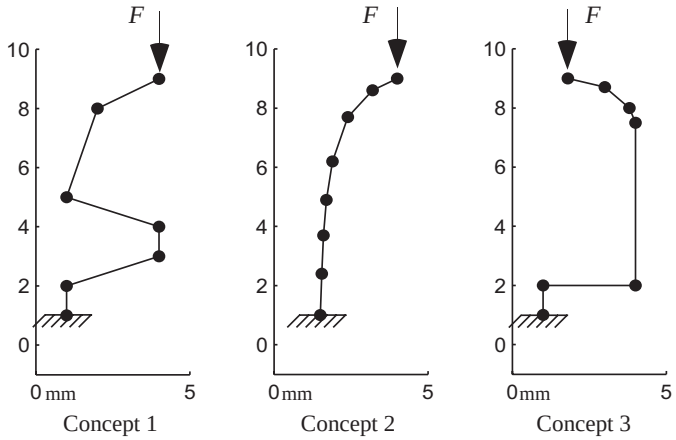

Figure 5: Simple structural representations for three battery contact concepts.

of the device. In contrast, the s-Pareto framework is designed to identify the full range of optimal behavior for the developed concept. The results presented shortly illustrate this.

4.2 Modelling and Analysis:

Any constant cross-section contact can be simplified to and modeled according to the approach shown here. For the development of generalized relationships, consider the simplified contact model shown in Fig. 4. Nodes labeled p_1 through p_9 represent key locations in the profile of the contact geometry (any number of nodes could be used); p_9 is where the contact is fixed, p_1 is the free end of the contact, and p_2 through p_8 are where bends occur in the beam geometry. Vectors ($\vec{v}_i$) between nodes represent straight beam segments. The applied forces Q and F_1 are also shown and expressed in vector form ($\vec{q}$, $\vec{f}_1$).

Geometric vector models for the three battery contact concepts considered in this case study are shown in Fig. 5. The profile of each contact is shown in a 5 mm by 10 mm space. The fixed condition is shown, and the vertically applied load is shown as acting at the free end of the contact.

By strain energy theorems, we find the deflection (due to bending) of beam segment i, in the direction of the load Q, to be

$$\delta_i = \int_0^{L_i} \frac{M_i(\partial M_i/\partial Q)}{EI} \, \mathrm{d}x_i \tag{12}$$

where L_i is the length of segment i, M_i is the moment in segment i, Q is an applied (or dummy) load, E and I are the modulus of elasticity and moment of inertia, and x_i is along the length of beam segment i.

The moment, M_i, in each beam segment comprises potentially two terms; (1) moments due to applied loads, and (2) a dummy moment caused by the dummy load. For the generic beam segment i, the total moment at x_i is

$$M_i = \Lambda_i|\vec{q}|\sin\alpha_i x_i + \Gamma_i|\vec{f}_1|\sin\beta_i x_i \tag{13}$$

where the first term is the moment due to the dummy load Q and the second term is the moment due to the applied load F_1. The terms Λ_i and Γ_i are scalars of value 1 or -1 and represent the direction of the moment created in segment i by the applied loads $\vec{q}$ and $\vec{f}_1$, respectively. Computationally, these directions, and therefore the scalars, are found using the vector cross product of $\vec{q}$ and $\vec{v}_i$, and of $\vec{f}_1$ and $\vec{v}_i$, respectively. $|\vec{q}|$ is the magnitude of the dummy load, α_i is the angle between the dummy load and beam segment i (obtained using the vector dot product), and β_i is the angle between the applied load $\vec{f}_1$ and beam segment i.

The total deflection of the contact at the point of, and in the direction of, the dummy load Q is the summation of all deflections δ_i, where $i \in 1, 2, ..., N$, and N is the number of beam segments. The generalized moment in Eq. 13 is also used to define the generalized bending stress (σ_i) in each segment.

4.3 Optimization Problem Statement:

The multiobjective optimization problem statement for obtaining the s-Pareto frontier for the set of concepts is given in the following.

Optimization Problem Statement for Battery Contact

$$\min_k \left\{ \min_{L^k} \left[-\delta^k \;\; \sigma^k_{\max} \right]^T \right\} \tag{14}$$

subject to

$$\delta^k = \sum_{i=1}^{N^k} \delta_i^k \tag{15}$$

$$\sigma^k_{\max} \leq \sigma_{\text{allowable}} \tag{16}$$

$$L^k_{il} \leq L^k_i \leq L^k_{iu} \qquad i = 1, ..., n^k_x \tag{17}$$

where

$$L^k = \left[L^k_1 \;\; ... \;\; L^k_{n^k_L} \right]^T \tag{18}$$

and k, $k \in \{1, 2, ..., n_c\}$, denotes the k-th concept, and L^k denotes the design variable vector for concept k. For this case study, the design variables (L) are the lengths of the

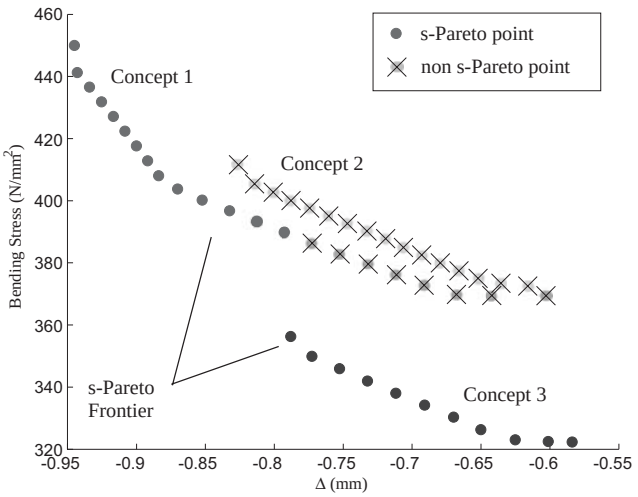

Figure 6: s-Pareto Frontier for Contact Concepts

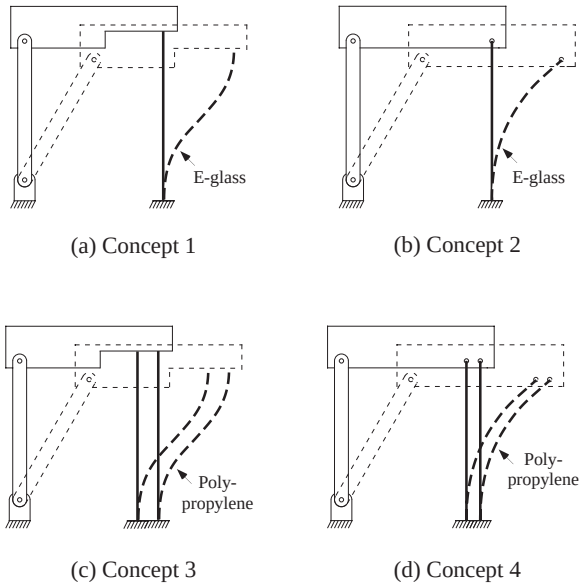

(a) Concept 1 (b) Concept 2

(c) Concept 3 (d) Concept 4

Figure 7: Compliant bicycle derailleur concepts.

beam segments, which we allow to expand or contract 20% of its initial length.

4.4 Results and Discussion:

A set of s-Pareto solutions that results from the problem statement provided above is shown as a set of solid circles in Fig. 6. For discussion purposes, we have also shown the individual Pareto sets for each concept. Once the s-Pareto frontier has been identified, the designer can examine it to draw important conclusions about the tradeoffs that exisit between the candidate concepts. Also, the designer can also draw conclusions about the tradeoffs that exist within a single concept.

The s-Pareto frontier immediately indicates that Concept 2 is dominated by Concepts 1 and 3. If the designer is comfortable with the objectives that he or she has modelled, then it can be concluded that Concept 2 should not be pursued. The remaining concepts comprise the s-Pareto frontier, and therefore the tradeoffs between these concepts are easily characterized. Concept 1 provides the maximum contact deflection (a characteristic that is highly desirable in connectors), however it comes at the cost of higher bending stresses. If the designer is satisfied with 0.79 mm deflection, the s-Pareto frontier indicates that Concept 3 can be chosen to meet the deflection need while developing significantly less bending stress in its members, when compared to Concept 1. These types of observations, which only come from examining the range of optimal behavior for each concept, provide the designer with insightful information that is likely to lead to a good concept selection decision.

Incidently, this study was carried out with a connector manufacturing company, and through this experiment, Concept 1 was selected because it provided the largest deflections in a sufficiently safe way. In subsequent developments, Concept 1 was detailed and modeled in a commercial CAD package, FEA was performed, prototypes were tested, and it is now mass produced for a leading mobile phone manufacturer.

5 Case Study 2: Compliant Bicycle Derailleur

This section considers the design of a bicycle derailleur. The purpose of this case study is to illustrate how the s-Pareto framework is executed for designs of more than two objectives. The basic derailleur design problem is presented below, followed by a description of the candidate derailleur concepts. We then provide the optimization problem statement for obtaining the s-Pareto sets for the derailleur case; the results and related discussion are then presented.

Derailleur Design Problem: Design a compliant bicycle derailleur that is lighter than a rigid-body derailleur of similar force-deflection characteristics. We note that a compliant derailleur is a four-bar mechanism that gains some or all of its motion through the large deflection of one or more of its links.

5.1 Candidate Derailleur Concepts:

As the initial steps in the conceptual design process, various compliant derailleur concept were generated. Specifically, twenty-eight possible design configurations for the compliant derailleur were identified using the Pseudo-Rigid-Body Model (PRBM) (27; 28) and type synthesis (29; 30). The PRBM allows compliant mechanisms to be modeled and analyzed as rigid-body mechanisms and significantly reduces the complexity of analysis. Using feasibility judgement, we reduce the set of twenty-eight designs down to two promising configurations. One of the configurations is shown in Fig. 7(b). This configuration comprises one compliant member (shown as a thin line), which has

Table 1: Material properties for derailleur case

Material	E (psi)	$S_{\max}$ (psi)	ρ (lbm/in^3)
E-Glass	1,430,000	260,000	0.0931
Polypropylene	800,000	24,000	0.0325

E = modulus of elasticity; $S_{\max}$ = max. bending stress; ρ = mass density

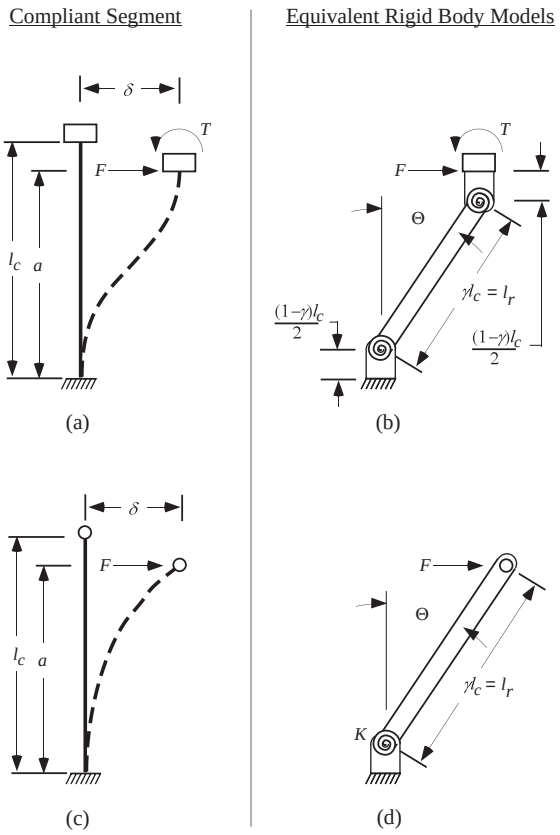

Figure 8: Pseudo-Rigid-Body Model (PRBM) for fixed-guided compliant segment (b). PRBM for fixed-free compliant segment (c).

one fixed end and one pinned end. A second configuration is shown in Fig. 7(a). This configuration also has one compliant member, however, both ends are fixed. The compliant link for Concepts 1 and 2 is an E-glass composite, while Concepts 3 and 4 use multiple strips of polypropylene for the compliant members. Concept 3 has 14 polypropylene strips (only two are shown in the figure), while Concept 4 has only two.

The overall goal is to identify the most promising derailleur concepts, based on the following design objectives; (i) minimize the mass of the compliant member, (ii) maximize the force required to deflect the mechanism (within reasonable bounds), and (iii) maximize the safety factor on bending stress in the compliant members.

5.2 Modeling and Analysis

The force and deflection characteristics of the compliant derailleur concepts are modeled using the PRBM (28). The fixed-guided beam in Fig. 8(a) is modeled under the PRBM approach as rigid links with torsional springs, as shown in Fig. 8(b). For the fixed-free beam shown in Fig. 8(c), the PRBM is given in Fig. 8(d).

The fixed parameters common to the four derailleur concepts are (i) deflection, $\delta = 1.5$ in, and (ii) the length of the rigid-body link (which needs to match a benchmark design), given as $l_r = 1.75$ in. The material properties used in this case study are given in Table 1. The geometrical relationships that are common to the four derailleur concepts are given as follows. The area moment of inertia is

$$I = \frac{bh^3}{12} \tag{19}$$

The length of the compliant member is

$$l_c = \frac{l_r}{\gamma} \tag{20}$$

The rigid-body angle, or the angle that the rigid link takes, is given by

$$\Theta = \arcsin \frac{\delta}{\gamma l_c} \tag{21}$$

The vertical position of the end of the beam is given as

$$a = l_c(1 - \gamma(1 - \cos\Theta)) \tag{22}$$

where the values for γ are provided in Table 2 (28), for each concept. Note that each concept has its own parametric model that characterizes the performance of design alternatives that belong to that concept's definition. Table 2 provides the details of the parametric models for the four concepts. Each column in the table represents a concept, and the rows represent values or relationships that are unique from concept to concept. Note that, in Table 2, ρ_1 is the density of the E-glass, whereas ρ_2 is the density of the polypropylene.

5.3 Optimization Problem Statement

The multiobjective optimization problem statement for the compliant bicycle derailleur design is given as

Optimization Problem Statement for Derailleur Design

$$\min_k \left\{ \min_{b^k, h^k} \begin{bmatrix} M^k & -F^k & -\mathcal{N}^k \end{bmatrix}^T \right\} \tag{23}$$

subject to

$$1.1 \leq \mathcal{N}^k \qquad \forall\ k \in \{1,2,3,4\} \tag{24}$$

$$5 \text{ lb} \leq F \leq 12 \text{ lb} \quad \forall\ k \in \{1,2,3,4\} \tag{25}$$

$$0.01 \text{ in} \leq b^k \leq 1 \text{ in} \quad \forall\ k \in \{1,2,3,4\} \tag{26}$$

$$0.01 \text{ in} \leq h^k \leq 0.05 \text{ in} \quad \forall\ k = 1,2 \tag{27}$$

Table 2: Concept Analysis for Derailleur Case Study

	Concept 1	Concept 2	Concept 3	Concept 4
γ	0.8517	0.85	0.8517	0.85
K_Θ	2.6762	2.68	2.6762	2.68
n_e	–	–	14	2
K^k	$\frac{2\gamma K_\Theta EI}{l_c}$	$\frac{\gamma K_\Theta EI}{l_c}$	$\frac{2n_e\gamma K_\Theta EI}{l_c}$	$\frac{n_e\gamma K_\Theta EI}{l_c}$
F^k	$\frac{4K^k\Theta}{\gamma l_c \cos\Theta}$	$\frac{K^k\Theta}{\gamma l_c \cos\Theta}$	$\frac{4n_eK^k\Theta}{\gamma l_c \cos\Theta}$	$\frac{n_eK^k\Theta}{\gamma l_c \cos\Theta}$
M^k	$bhl_c\rho_1$	$bhl_c\rho_1$	$n_ebhl_c\rho_2$	$n_ebhl_c\rho_2$
S^k	$\frac{F^kah}{4I}$	$\frac{F^kah}{2I}$	$\frac{F^kah}{4n_eI}$	$\frac{F^kah}{2n_eI}$
$\mathcal{N}^k$	$\frac{S_{\max}}{S^k}$	$\frac{S_{\max}}{S^k}$	$\frac{S_{\max}}{S^k}$	$\frac{S_{\max}}{S^k}$

K^k = stiffness of mechanism; M^k = mass of compliant member, S^k = bending stress, F^k=output force; $\mathcal{N}^k$ = safety factor

$$0.005 \text{ in} \leq h^k \leq 0.05 \text{ in} \quad \forall\ k = 3, 4 \tag{28}$$

As can be seen in the problem statement, we minimize the mass (M), maximize the force (F) within limits, and maximize the safety factor ($\mathcal{N}$). In the next section, the s-Pareto frontier that results from this problem statement is provided, and the interactive exploration approach, described in Sec. 3, is used to explore the s-Pareto frontier and characterize the goodness of the concepts.

5.4 Results and Discussion

The top plot in Fig. 9 shows Pareto sets for each derailleur concept. The Pareto sets were obtained using the Normal Constraint Method (31). The center plot in Fig. 9 shows the s-Pareto set that originates from the Pareto sets of each concept. Immediately, it can be seen that Concepts 3 and 4 are not part of the s-Pareto set. This is because they are dominated concepts. We make the important note that we have identified these concepts as dominated only after we have explored the objectives behaviors over ranges – an approach that is markedly different from traditional concept selection approaches where objectives ranges are not typically considered. Because Concepts 3 and 4 are dominated they can be removed from the set of candidate designs.

It can also be observed that a small portion of the Pareto set for Concept 1 has been removed, indicating that parts of this concept are dominated by Concept 3. In contrast to the battery contact case study presented in the previous section, the tradeoffs between the remaining concepts are not easily observed by inspecting the plot.

We can, however, use the interactive s-Pareto frontier exploration tool, developed in Mattson and Messac (11), to identify the dominance disposition of each concepts. With each exploration, the measure of concept goodness is evaluated (see Eqs. 10 and 11). Its worth noting that when using Eq. 11 to evaluate concept goodness, the evaluation is instantaneous from a practical point of view, thus enabling as many explorations as the designer deems necessary.

Without exception, we have observed that designers make the following inquiries during the exploration process; (i) which concept optimizes objectives 1, which concept optimizes objective 2, and so on; (ii) when considering the complete feasible space, which concept covers the greatest space? For this case study, these inquiries result in the following: Concept 1 provides the minimal mass. Concept 1 provides the largest actuation force. Concept 3 provides the largest safety factor on bending stress. When considering the complete feasible space, Concept 1 covers 54.8% of the space, while Concept 3 covers 45.2%.

Other custom scenarios are typically explored by the designers. For example, after obtaining the s-Pareto frontier, the designer may express preference to have a safety factor greater than 2.5, an actuation force of at least 8 lbf, and that any mass as long as its in the feasible region would be desired. To explore the goodness of each concept within the context of this scenario, the designer uses the interactive tool by selecting the point (2.421e-3, -8, -2.5) for (Mass, Actuation Force, Safety Factor). Doing this evaluates the candidate concepts only in the region that dominates this point. Because it is where the designer would prefer the selected design to reside, this region is termed

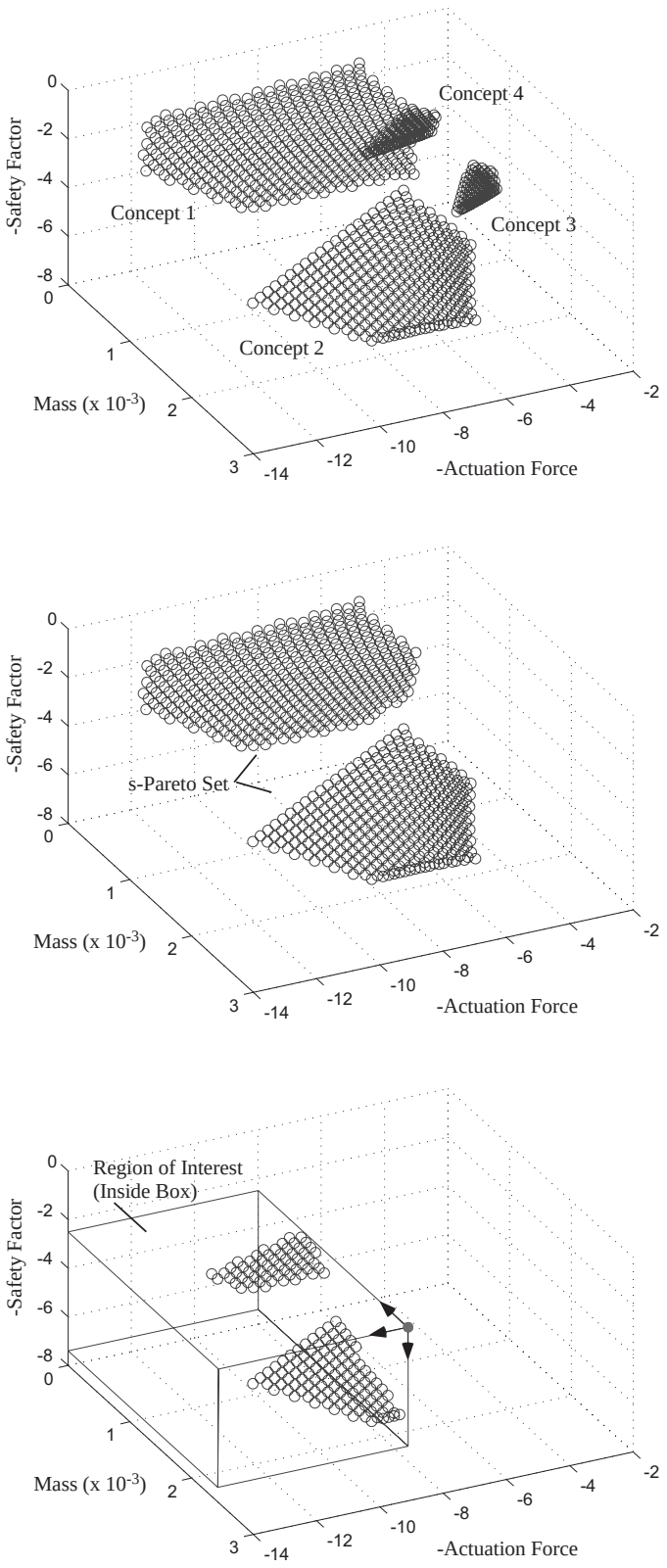

Figure 9: (top) Pareto sets for each concept, (center) an s-Pareto set for the compliant bicycle derailleur concepts, (bottom) a region of interest wherein the goodness of each concept is considered.

the Region of Interest. The bottom plot in Fig. 9 shows the region of interest for this scenario, and the s-Pareto points considered when evaluating the goodness of the concepts. For this scenario, Concept 3 is found to cover more of the space (64.7%).

By exploring various regions of interest the designer can more easily characterize the location of the concepts within the design space. This characterization enables the designer to make informed concept selection decision without explicitly seeing the s-Pareto frontier.

A recent publication by Mattson et al. (32) highlights the selected derailleur design as a commercially feasible compliant mechanism due to its low mass – a critical objective for high-performance cycling. The publication provides pictures of a manufactured compliant bicycle derailleur.

6 Case Study 3: Rigidified Inflatable Structures

In this section, we use the s-Pareto framework for the material selection of a large-scale structural system. Specifically, our case study examines the design of a Rigidified Inflatable Structure (RIS) (33). The purpose of this case study is to show that the s-Pareto frontier can be used to evaluate complex systems, and that (depending on the nature of the design problem) a minimal number of s-Pareto solutions can be obtained and used to approximate the s-Pareto frontier.

Rigidified Inflatable Structures are initially *flexible* thin membranes that transform into *rigid* load bearing structures after undergoing pneumatic deployment. These structures were initially developed for applications in the space industry, where it is critical that structures possess small stowed volume for ease of transport. Recently, Van Dessel et al. (34), and Messac et al. (33) have discussed the use of a RIS for residential construction. Van Dessel et al. (34) present a RIS design where the walls are arrays of tubular bays; they specifically explore the effect of bay size on the feasibility of the residential structure. Messac et al. (33) report on the performance of a representative cylindrical RIS housing structure under the effect of typical housing loads, such as roof load and wind load.

In this case study, we demonstrate that the s-Pareto approach is not restricted to concept selection problems, but that it is useful for decision making in general. In this case study, we use the s-Pareto frontier to evaluate and select materials for the RIS housing structure described in Messac et al. (33). Specifically, the design problem is stated below.

RIS Design Problem: From a set of three candidate RIS materials, identify a material that best satisfies the design requirements for the deployed RIS model specified in Messac et al. (33). As we will see in the following sections, the s-Pareto framework is well-suited for such a design problem.

In Messac et al. (33), this same design problem was addressed under a different strategy. The best material

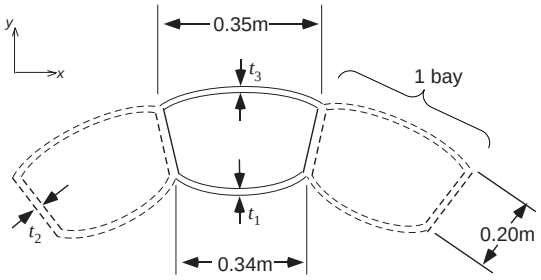

Figure 10: Top view crosssection for three bays of a cylindrical rigidified inflatable structure

was selected by obtaining one optimization solution for each material, and comparing the optimal values of the objectives. A decision made using only one Pareto optimal design for each material may not, however, truly reflect the tradeoffs between the materials for different values of the objectives. In the present case study, we perform the material selection for the RIS by obtaining solutions on the s-Pareto frontier. For this material selection problem, the "concepts" are the different RIS materials. Using these s-Pareto solutions, we make key decisions regarding which material merits further consideration for use in residential RIS designs.

The following section describes the RIS model employed, and the analysis approach. The optimization problem statement and approach are then presented, followed by the results and discussion.

6.1 Modeling and Analysis

The model described in Messac et al. (33) is used in this case study. The model is a cylindrical building with a floor area of 192 m^2, and a height of 3 m. The wall is 0.2 m thick, and is made of tubular columns. Each column, or bay, comprises four thin membranes, as depicted in Fig. 10. Adjacent bays share a common side membrane, which remains straight after inflation, due to equal and opposite pneumatic pressures from either side. The other two membranes (interior and exterior) protrude outward due to the inflation pressure, as shown in Fig. 10. The structure is subjected to a roof load of 4000 N/m on the top (z-direction), and a wind load of 1000 N/m^2 on one side of the cylindrical structure (in the y-direction).

Finite Element Model

The above structure is modeled using Genesis (35), a finite element and optimization program. The entire structure is modeled using four-noded plate elements with in-plane and bending stiffness. The total number of elements and nodes for the model are 12960 and 12672 nodes, respectively. The structure is constrained such that all the nodes at the bottom are assumed to be pinned to the foundation, while all the remaining nodes are unconstrained. These structural constraints result in a total of 72,576 degrees of freedom.

Figure 11 shows the results of a preliminary analysis performed on the model. It shows the deformed shape and the stress contours.

Table 3: Material properties for the RIS design

Material Class	E (GPa)	$\sigma_{\max}$ (MPa)	ρ (kg/m^3)	c ($/kg)
1	3.0	30.0	1400	2.50
2	10.0	100.0	1900	11.00
3	30.0	300.0	2100	22.00

E = modulus of elasticity; $\sigma_{\max}$ = tensile strength; ρ = mass density; c = cost

Material Properties

For this case study, we consider three candidate material classes for the RIS design. Table 3 shows the properties for each material class. The three material classes are : (i) non-reinforced polymers, (ii) polymers lightly reinforced with randomly oriented, discontinuous E-glass fibers, and (iii) polymers reinforced with uniform, continuous E-glass fibers.

From Table 3, it is not immediately clear which material will be the most cost efficient, or which material will effectively support the loads applied, while satisfying the design requirements. A single analysis and optimization will not entirely reveal the tradeoffs between the materials. This situation necessitates the use of more involved techniques to make critical decisions. We propose to use an optimization based framework – the s-Pareto approach – to select the optimal material properties for RIS. The next section discusses the details of the optimization problem.

6.2 Optimization Problem Statement and Procedure

In this section, we describe the optimization problem that is solved for each material. We then discuss the approach that we use to obtain individual points on the Pareto frontier for each material.

We consider two design objectives as part of the multi-objective optimization problem: (i) Cost (c): Material cost plays an important role in the design of any system. From Table 3, we can see that there is a significant difference between the cost of each material, indicating the possibility of significant tradeoff. For simplicity, we only consider material cost for the RIS structure, and assume that all other costs are approximately the same. We seek to minimize the material cost as part of the optimization process. (ii) Deflection (δ_y): We minimize the deflection produced in the structure as a result of the applied loads. Primarily, we focus on the deflection in the y-direction (the direction of the wind load) because it is more significant than the deflection along the other axes, and hence we choose it be our second design objective. We note that although only two objectives are considered here, the material selection process presented here can be readily used for more than two dimensions.

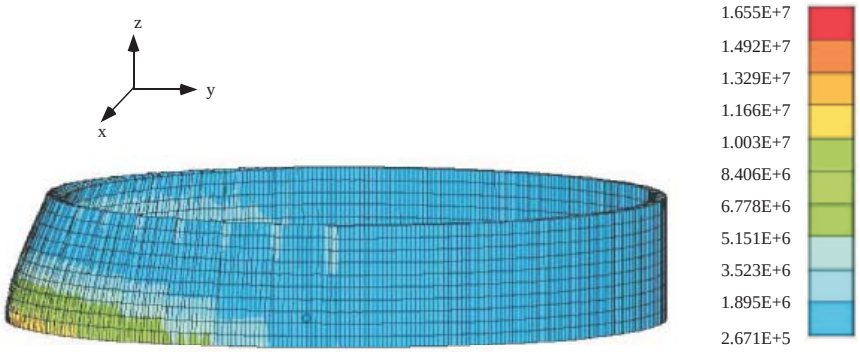

Figure 11: Deformed shape and stress contours under the action of applied loads

The design variables are the thicknesses of the various membranes. These are t_1, t_2, and t_3 – the thicknesses of the interior, side, and exterior membranes, respectively. Figure 10 shows these dimensions.

The stress in the structure is constrained to be less than the allowable stress for the particular material after applying a factor of safety of 2. The deflection in the direction of the wind is constrained to be less than the allowable deflection of 6 cm.

These details are incorporated in the following optimization problem statement.

Optimization Problem Statement for the RIS Design

$$\min_{t_1^k, t_2^k, t_3^k} \quad [\ c^k \quad \delta_y^k\ ]^T \tag{29}$$

subject to

$$\sigma^k \leq \frac{\sigma_{\max}^k}{2} \tag{30}$$

$$\delta_x^k \leq 6 \text{ cm} \tag{31}$$

$$\delta_y^k \leq 6 \text{ cm} \tag{32}$$

$$t_{\min} \leq t_1^k,\ t_2^k,\ t_3^k \leq t_{\max} \tag{33}$$

where the superscript k denotes the quantities associated with the k-th material, c^k denotes the structural cost using material k, δ_y^k denotes the structural deflection when using material k, σ^k represents the stress response value in the structure for the k-th material, and $\sigma_{\max}^k$ denotes the yield strength of the k-th material. Finally, t_1^k, t_2^k, t_3^k denote the design variables for the k-th material.

6.3 Optimization Approach

The above problem statement (Eqs. 29–33) represents the multiobjective optimization problem that yields the Pareto frontier for the k-th material. The RIS model discussed above has over 72000 degrees of freedom, and requires over an hour to compute a single Pareto solution on a single 600 MHz processor. In such cases, it may not be practical to obtain a large number of points on the Pareto frontier of each material. We can instead follow one of these approaches: (i) generate approximate analytical functions of the actual model using the response surface methodology or, (ii) intelligently solve the multiobjective optimization problem to obtain only a small representative set of Pareto optimal solutions using the actual model, and then interpolate the other Pareto solutions using the previously obtained solutions. For this case study, we follow the latter approach, since the former can be more computationally expensive, especially for problems that involve multiple objectives (36).

There are several methods to obtain Pareto optimal solutions, such as (i) formation of an Aggregate Objective Function (AOF): weighted sum, compromise programming, (ii) transforming the multiobjective problem into a single objective problem: normal constraint method (6), normal boundary intersection method (37), and so on. The approach that we have used in this case study follows the ε-inequality constraint methodology (38). Under this approach we transform the bi-objective problem into a single objective problem, and constrain the second objective to be less than or equal to a carefully chosen value. Solving the single objective problem using the Genesis optimizer yields a Pareto optimal solution. By judiciously choosing the pre-determined value, we can obtain different Pareto optimal solutions. By smart choices of this value, we can obtain a fairly accurate representation of the actual Pareto frontier (for example, see Fig. 12).

After obtaining the Pareto frontiers for the individual materials, we identify the s-Pareto frontier for the three materials. The s-Pareto frontier characterizes which materials perform better than the other materials in different situations. The following section presents these results.

6.4 Results and Discussion

Using the approach discussed in the previous section to obtain individual Pareto optimal solutions for the three materials, we obtain the results shown in Fig. 12. The markers represent the individual Pareto optimal solutions, and the approximate Pareto frontier is shown as a line joining these points. The Pareto frontiers for the three materials are shown as thin lines, while the s-Pareto frontier for

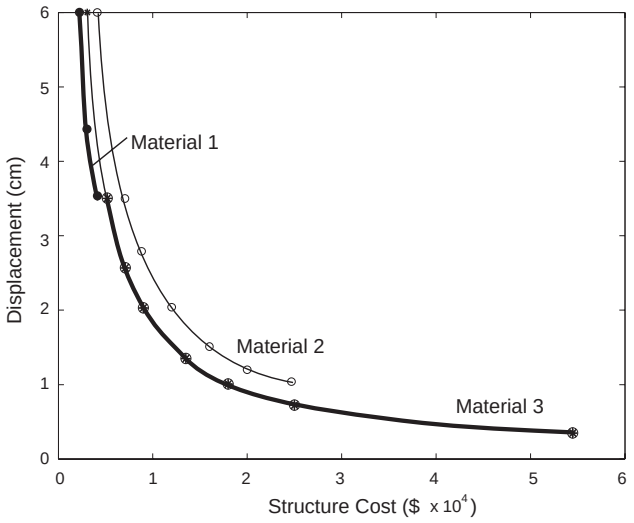

Figure 12: Approximate s-Pareto frontier (bold) for the three materials

all the three materials is shown as a bold line.

We can see from Fig. 12 that for the two design objectives considered – cost and deflection – Material 2 is a dominated material, that is, no point on the Pareto frontier of Material 2 dominates the Pareto points of Material 1 or 3. Hence, no part of Material 2 belongs to the s-Pareto frontier of the three materials. Between Materials 1 and 3, there exists a tradeoff between the objectives of minimizing cost and deflection. For low values of cost (less than $4000), only Material 1 contributes to the s-Pareto frontier, while for low values of deflection (less than 3.5 cm), only Material 3 contributes to the s-Pareto frontier. Thus, Material 1 can be considered to be the optimal material for low cost structures, whereas Material 3 is optimal for small deflection. The s-Pareto frontier further quantifies these cost and deflection values, and depending on the preferences specified by the designer, he or she can choose the appropriate material.

7 Concluding Remarks

This paper has investigated three real-world applications of the newly-developed s-Pareto frontier based concept selection framework. The new framework was specifically shown to facilitate the characterization of design tradeoffs between (i) conflicting design objectives, and (ii) competing design concepts. As such, the new framework indeed holds significant potential for use in concept selection and decision-making in general.

The first case study highlighted the design of a battery contact for a mobile phone. The purpose of this study was to show (i) the basic workings of the s-Pareto framework, and (ii) the role that the s-Pareto frontier has in the conceptual design process. Importantly, the s-Pareto frontier aided designers in selecting a design that was later detailed using CAD, FEA, and prototype testing.

In the second case study, we examined the design of a compliant bicycle derailleur. The selection process began with 28 generic derailleur configurations. Four derailleur concepts were generated from the most promising generic configurations. The obtained s-Pareto frontier for these concepts showed that two of the four concepts did not merit further consideration. An approach for exploring s-Pareto frontiers was used to characterize the tradeoffs between the remaining two concepts.

In the third case study, the design of a rigidified inflatable structure was considered. Specifically, we used the s-Pareto frontier to facilitate the RIS material selection problem. Three candidate materials were evaluated using a conceptual RIS model developed by Messac et al. (33). Because the RIS model was computationally expensive to evaluate, we judiciously obtained a minimal number of solutions on the s-Pareto frontier. After carefully obtaining a minimal set, the s-Pareto frontier was identified and used to characterize the tradeoffs between the objectives and the tradeoffs between the materials. One material was shown to be dominated, while the other two materials showed different advantages in their own respect. This case study showed that (i) the s-Pareto frontier can be useful for problems involving computationally intensive models, (ii) the s-Pareto framework can be used under various implementation strategies, and (iii) the s-Pareto frontier holds significant potential for decision-making in general.

In each cases, the s-Pareto frontier was used to facilitate the designer's important responsibility of identifying design tradeoffs and navigating through the design options to select designs that merit further development.

8 Acknowledgements

This research was supported by National Science Foundation Grants DMI-0196243 and DMI-0354733 for Achille Messac.

REFERENCES

[1] Miettinen, K. M., *Nonlinear Multiobjective Optimization*, International Series in Operations Research & Management Science, Kluwer Academic Publishers, 1999.

[2] Belegundu, A. and Chandrupatla, T., *Optimization Concepts and Applications in Engineering*, Prentice Hall, New Jersey, 1999.

[3] Steuer, R. E., *Multiple Criteria Optimization, Theory Computations and Applications*, John Wiley & Sons, Inc., New York, 1986.

[4] Balling, R. J., "Pareto Sets in Decision-based Design," *Engineering Valuation and Cost Analysis*, Vol. 3, 2000, pp. 189–198.

[5] Messac, A. and Mattson, C. A., "Generating Well-Distributed Sets of Pareto Points for Engineering Design using Physical Programming," *Optimization and Engineering*, Vol. 3, December 2002, pp. 431–450, Kluwer Publisher.

[6] Messac, A., Ismail-Yahaya, A., and Mattson, C. A., "The Normalized Normal Constraint Method for Generating the Pareto Frontier," *Structural and Multidisciplinary Optimization*, Vol. 25, No. 2, 2003, pp. 86–98.

[7] Ulrich, K. T. and Eppinger, S. D., *Product Design and Development*, chap. 7, McGraw-Hill, Inc., Boston, 2nd ed., 2000, pp. 138–159.

[8] Ullman, D. G., *The Mechanical Design Process*, chap. 9, McGraw-Hill, Inc., 1992, pp. 168–184.

[9] Akao, Y., *Quality Function Deployment: Integrating Customer Requirements into Product Design*, Productivity Press, 1990, Translated by Glenn H. Mazur.

[10] Pugh, S., *Creating Innovative Products Using Total Design: The Living Legacy of Stuart Pugh*, chap. 14 and 15, Addison-Wesley, Reading, MA, 1st ed., 1996, pp. 167–182, with contributions by Don Clausing and Ron Andrade.

[11] Mattson, C. A. and Messac, A., "Pareto Frontier Based Concept Selection Under Uncertainty, with Visualization," *Optimization and Engineering*, Vol. 6, No. 1, 2005, pp. 85–115, Invited Paper, Special Issue of Multidisciplinary Design Optimization.

[12] Ramaswamy, V., Lewis, K. E., Sundararaj, G. J., and Messac, A., "Discrete Subsystem Selection Using Linear Physical Programming," Proceedings of the 1999 AIAA/ASME/ASCE/AHS/ASC Structures, Structural Dynamics, and Materials Conference and Exhibit, 1999.

[13] Crossley, W. A., Martin, E. T., and Fanjoy, D. W., "Conceptual Aircraft Design Environment: Case Study Evaluation of Computing Architecture Technologies," 1st AIAA Aircraft, Technology, Integration, and Operations Forum, Paper Number AIAA 2001-5247, 2001.

[14] Perez, R. E., Chung, J., and Behdinan, K., "Aircraft Conceptual Design Using Genetic Algorithms," 8th AIAA/USAF/NASA/ISSMO Symposium on Multidisciplinary Analysis and Optimization, Paper Number AIAA 2000-4938, 2000.

[15] Simpson, T. W., *A Concept Exploration Method for Product Family Design*, Ph.D. thesis, The George W. Woodruff School of Mechanical Engineering, Georgia Institute of Technology, Atlanta, GA, 1998.

[16] Pedersen, K., *Designing Platform Families: An Evolutionary Approach to Developing Engineering Systems*, Ph.D. thesis, The George W. Woodruff School of Mechanical Engineering, Georgia Institute of Technology, Atlanta, GA, 1999.

[17] Messac, A., Martinez, M., and Simpson, T., "Effective Product Family Design Using Physical Programming," *Engineering Optimization*, Vol. 34, No. 3, 2002, pp. 245–261.

[18] Messac, A., Martinez, M., and Simpson, T., "Introduction of a Product Family Penalty Function Using Physical Programming," *ASME Journal of Mechanical Design*, Vol. 124, No. 2, 2002, pp. 164–172.

[19] Yang, R. J., Chuang, C.-H., and Che, X., "Recent Applications of Topology Optimization," 7th AIAA/USAF/NASA/ISSMO Symposium on Multidisciplinary Analysis and Optimization, Paper Number AIAA 98-4849, 1998.

[20] Mattson, C. A. and Messac, A., "Concept Selection Using s-Pareto Frontiers," *AIAA Journal*, Vol. 41, No. 6, 2003, pp. 1190–1198.

[21] Crossley, W. A. and Laananen, D. H., "Conceptual Design of Helicopters via Genetic Algorithm," *Journal of Aircraft*, Vol. 33, No. 6, Nov–Dec 1996, pp. 1060–1070.

[22] Simpson, T. W., Rosen, D., Allen, J. K., and Mistree, F., "Metrics for Assessing Design Freedom and Information Certainty in the Early Stages of Design," *ASME Journal of Mechanical Design*, Vol. 120, 1998, pp. 628–635.

[23] DeLaurentis, D. A., Cesnik, C. E. S., Mavris, D. N., and Schrage, D. P., "A New Approach to Integrated Wing Design in Conceptual Synthesis and Optimization," Proceedings of the 6th AIAA/NASA/ISSMO Symposium on Multidisciplinary Analysis and Optimization, AIAA Paper No. AIAA 96-4000, 1996.

[24] Giesing, J. P. and Barthelemy, J.-F. M., "A Summary of Industrial MDO Applications and Needs," MDO technical committee report, AIAA MDO Technical Committee, 1998.

[25] Mattson, C. A. and Messac, A., "A Non-Deterministic Approach to Concept Selection Using s-Pareto Frontiers," ASME 2002 Design Engineering Technical Conference and Computers and Information in Engineering Conference, Design Automation Conference, Montreal, Canada, September 2002.

[26] Mattson, C. A., *A New Paradigm for Concept Selection in Engineering Design Using Multiobjective Optimization*, Ph.D. thesis, Department of Mechanical, Aerospace, and Nuclear Engineering, Rensselaer Polytechnic Institute, Troy, NY, 2003.

[27] Howell, L., Midha, A., and Norton, T. W., "Evaluation of Equivalent Spring Stiffness for Use in a Pseudo-rigid-body Model of Large-Deflection Compliant Mechanisms," *ASME Journal of Mechanical Design*, Vol. 118, 1996, pp. 125–131.

[28] Howell, L. L., *Compliant Mechanisms*, John Wiley & Sons, New York, NY, 2001.

[29] Derderian, J. M., Howell, L. L., Murphy, M. D., Lyon, S. M., and Pack, S. D., "Compliant Parallel-Guiding Mechanisms," Proceedings of the ASME Design Engineering Technical Conferences, DETC-1996-MECH-1208, 1996.

[30] Murphy, M. D., Midha, A., and Howell, L., "The Topological Synthesis of Compliant Mechanisms," *Mechanism and Machine Theory*, Vol. 31, No. 2, 1996, pp. 185–199.

[31] Messac, A. and Mattson, C. A., "Normal Constraint Method with Guarantee of Even Representation of Complete Pareto Frontier," *AIAA Journal*, Vol. 42, 2004, pp. 2101–2111.

[32] Mattson, C. A., Howell, L. L., and Magleby, S. P., "Development of Commercially Viable Compliant Mechanisms Using the Pseudo-Rigid Body Model: Case Studies of Parallel Mechanisms," *Journal of Intelligent Material Systems and Structures*, Vol. 15, No. 3, 2004, pp. 195–202.

[33] Messac, A., Dessel, S. V., Mullur, A. A., and Maria, A., "Optimization of Large-Scale Rigidified Inflatable Structures for Housing Using Physical Programming," *Structural and Multidisciplinary Optimization*, Vol. 26, No. 1-2, 2004, pp. 139–151.

[34] Van Dessel, S., Messac, A., Mullur, A., and Farina, A., "Feasibility and Optimization of Rigidified Inflatable Structures for Housing," *ASCE Journal of Structural Engineering*, Vol. 129, No. 11, 2003, pp. 1494–1502.

[35] Vanderplaats, G. N., *Genesis Structural Analysis and Optimization*, Vanderplaats Research and Development, 2001, Version 7.0.

[36] Koch, P. N., Simpson, T. W., Allen, J. K., and Mistree, F., "Statistical approximations for multidisciplinary design optimization: the problem of size," *Journal of Aircraft*, Vol. 36, No. 1, 1999, pp. 275–286.

[37] Das, I. and Dennis, J., "A Closer Look at Drawbacks of Minimizing Weighted Sums of Objective for Pareto Set Generation in Multicriteria Optimization Problems," *Structural Optimization*, Vol. 14, 1997, pp. 63–69.

[38] Palli, N., Azarm, S., McCluskey, P., and Sundararajan, R., "An Interactive Multistage ϵ-Inequality Constraint Method for Multiple Objectives Decision Making," *ASME Journal of Mechanical Design*, Vol. 120, December 1998, pp. 678–686.